

# Towards an Understanding of the Transient Behavior of the Five-Parameter Iwan-Type Model

Lacayo<sup>1</sup>, Robert M., and Allen<sup>2</sup>, Matthew S.

<sup>1</sup>Engineer, ATA Engineering, Inc., 13290 Evening Creek Dr. S., San Diego, CA 92128

<sup>2</sup>Professor, University of Wisconsin - Madison, 1500 Engineering Dr, Madison, WI 53711

## ABSTRACT

Mignolet (2015, *Journal of Sound and Vibration*, 349, pp. 289-298) demonstrated mathematically that his proposed five-parameter Iwan-type model weakens the coupling between the change in effective stiffness and change in effective damping of the model as vibration amplitude changes. Several experimental studies on bolted-joint structures have experienced difficulty in fitting a traditional Iwan model to match measurements, so this advantage is sorely needed. However, Mignolet's work only considered steady-state harmonic motion, and the stiction behavior of the internal sliders was not studied in great detail. In this work, the force-constitutive formulation of the five-parameter Iwan-type model is implemented computationally and then examined to understand its behavior in more general transient scenarios. The five-parameter model is found to have a complicated dependence on its displacement history. If the model reaches a maximum steady-state displacement after a ring-up response (such as occurs when the system is excited at resonance by a shaker), the stiffness and damping it exhibits is consistent with those formulated by Mignolet. When the vibration decays below the maximum-achieved displacement, however, the effective stiffness and damping revert to power-law behavior with amplitude. The power-law behavior is functionally similar to that of the four-parameter Iwan model (on which the five-parameter model is based), so the advantage of the weakened coupling between the stiffness and damping is lost in a ring-down response.

**Keywords:** Iwan model, microslip, hysteresis, friction, nonlinear damping

## 1 INTRODUCTION

A well-known model for microslip is the parallel-series distributed-element model developed by Iwan [1]. This model consists of a parallel arrangement of a large (ideally infinite) number of Jenkins elements (a spring and Coulomb slider in series), where each Jenkins element has the same spring stiffness and slips at a different force. As the Iwan model displaces from equilibrium, each of the sliders begins to slip one after another. Segalman later defined a four-parameter distribution function that gives the force at which each Jenkins element slips, such that the energy dissipated per cycle by the Iwan model undergoing harmonic motion follows a power-law trend with the loading amplitude [2], as observed in many experiments [3, 4, 5, 6, 7, 8].

The four-parameter Iwan model strongly couples the stiffness with the dissipation, and this sometimes makes it challenging to fit the model to experimental measurements. Mignolet [7] investigated this problem and proposed allowing each slider to have different static and dynamic friction coefficients. This allows each slider to exhibit stiction: a large static friction force that decreases when the slider begins to move. Mignolet assigned a fifth parameter to govern this decrease in the friction force, and he used his new five-parameter Iwan-type formulation to derive closed-form expressions for amplitude-dependent stiffness and dissipation during steady-state harmonic motion. With these expressions, he was able to fit his model to stiffness and dissipation measurements successfully. However, Mignolet never investigated how the five-parameter Iwan-type model could be implemented for transient vibration, so the simplified expressions that he developed have not yet been verified, nor has anyone studied the implications of the fifth parameter on the transient response of a system with an Iwan joint.

This work presents an implementation of the five-parameter Iwan-type model and documents an investigation on the amplitude-dependent stiffness and dissipation of that element in more general transient settings. The results show that the five-parameter model has a complicated dependence on the past history of its displacement, especially on the largest displacement the joint has experienced. As a result, the behaviors that Mignolet discussed would only be observed if a virgin structure were excited monotonically up to the steady-state conditions that he assumed. In contrast, in a response where the amplitude decreases with time, the power-law behavior becomes functionally equivalent to that of the four-parameter model, so the advantage of weakened coupling between the stiffness and damping is lost. This study highlights how difficult it is to account for stiction when studying the vibration of joints and the additional implications that this presents, which should be addressed by future models.

## 2 OVERVIEW OF THE FIVE-PARAMETER IWAN-TYPE MODEL

An Iwan element consists of an infinite number of sliders that all slip at different force levels, as described by a distribution function,  $\rho(\phi)$ . The force in the Iwan element is a summation over these sliders [2] as follows,

$$F(t) = \int_0^{\infty} \Gamma(t, \phi) \rho(\phi) d\phi, \quad (1)$$

where

$$\Gamma(t, \phi) = \begin{cases} u(t) - x(t) & \text{for } |u(t) - x(t)| < \phi \text{ (sticking),} \\ \phi & \text{otherwise (slipping),} \end{cases} \quad (2)$$

tracks the current deflection,  $x$ , of each spring. The distribution function,  $\rho(\phi)$ , defined in [2], is chosen so that the Iwan element dissipates energy according to some power of the displacement amplitude, i.e. the log damping vs. log vibration amplitude is linear with a slope corresponding to the power-law exponent.

If the displacement of the five-parameter Iwan-type model is defined with a sinusoidal function, as in  $u(t) = u_0 \sin(\Omega t)$ , then Mignolet shows that the force exerted by the model while in microslip ( $u_0 < \phi_{\max}$ ) reaches a peak amplitude of [7]

$$F_0(u_0) = K_T u_0 - \Lambda u_0^{\chi+2}, \quad (3)$$

$$K_T = \frac{R \phi_{\max}^{\chi+1}}{(\chi+1)} + S, \quad \Lambda = \frac{R [\chi+2 - \theta(\chi+1)]}{(\chi+1)(\chi+2)}. \quad (4)$$

These expressions were then used to predict the tangent stiffness and energy dissipation of his five parameter Iwan element, resulting in the equations given in [7]. However, in that work a computational element was never developed, so the transient response of Mignolet's five-parameter model was never explored.

To investigate the transient behavior of a five-parameter Iwan-type model, a computational element embodying its force-constitutive relationship was created. Here the constitutive model is approximated by using a finite number of sliders, as done in [2], and assigning a slip threshold to each Jenkins element so that the integral in Eq. (1) becomes a summation. Also, an additional variable had to be added to track the state of each slider, whether stuck or slipping. Further details will be provided in the presentation.

### 3 THE TRANSIENT BEHAVIOR OF THE FIVE-PARAMETER IWAN-TYPE MODEL

The hysteresis of the Iwan-type element was observed in three different cases. The first case considered is the steady-state response of the element after virgin loading. This case matches that used by Mignolet when deriving Eq. (3). The remaining two cases examine the hysteresis in response to ring-up and ring-down deflection.

#### 3.1 Steady-State Behavior After Virgin Loading

An Iwan element with parameters  $\chi = -0.6$ ,  $\phi_{\max} = 6 \times 10^{-4}$ ,  $R = 7 \times 10^5$ ,  $S = 9 \times 10^3$  and  $\theta = 0.3$  was used. The element was discretized into a set of  $N = 10000$  sliders (many more than typical to ensure a smooth  $F_J$  approximating a continuous Iwan-type element). The discrete element was subjected to a sinusoidal deflection of the form

$$u(t) = u_0 \sin(2\pi t) \quad (5)$$

for one and one-quarter cycles ( $t \in [0, 1.25]$ ) sampled at step size 0.001. The element was displaced to an amplitude  $u_0 = 5 \times 10^{-4}$ . The slider states were first initialized to zero, i.e. a virgin structure. The resulting force-deflection curve is plotted in Fig. 1a. The first quarter cycle creates an initial loading curve up to  $u_0$ , and the remaining full cycle forms the reverse and forward curves of a hysteresis bounded by  $\pm u_0$ .

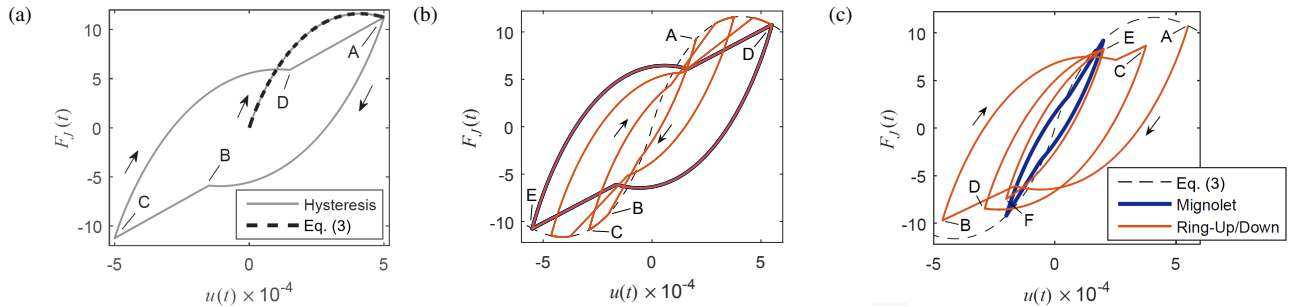


Figure 1: Force-deflection curves for the discrete Iwan-type element in the case of (a) sinusoidal displacement, (b) ring-up, and (c) ring-down force-displacement curves for  $\theta = 0.3$ .

While not elaborated here, one can use this result to show that if the Iwan-type element is loaded monotonically up to a certain displacement and then undergoes steady-state vibration at that amplitude, then the hysteresis it exhibits has a secant slope and enclosed area that is consistent with Mignolet's expressions for amplitude-dependent stiffness and dissipation. A hysteresis that exhibits this property is referred to as a "Mignolet hysteresis" in the rest of this work.

### 3.2 Ring-Up and Ring-Down Behavior

Two different sinusoidal displacement signals were constructed: one for the ring-up and the other for the ring-down. The ring-up signal was designed so that the amplitude increases linearly from a low boundary,  $u_L = 2 \times 10^{-4}$ , to a high boundary,  $u_H = 5.5 \times 10^{-4}$ , in two cycles, and then completes another cycle at the high boundary. The third cycle is meant to create a complete hysteresis loop for comparison with the Mignolet hysteresis at the final amplitude. Similarly, the amplitude of the ring-down signal was designed to change from  $u_H$  to  $u_L$  in two cycles followed by one cycle at  $u_L$ . The slider states in the two cases were initialized to account for the element having already displaced from zero to its starting location on the virgin loading curve.

The resulting force-deflection curves are shown in Fig. 1. For the ring-up curve (Fig. 1b), each forward and reverse path starts on the initial loading curve (point A) and proceeds to the opposite displacement (point B) by following the path of a Mignolet hysteresis. After reaching that displacement, the path of initial loading is followed until load reversal (point C). The third cycle (D to E to D) exactly traces the Mignolet hysteresis loop associated with the highest-achieved amplitude.

The ring-down force-deflection curve (Fig. 1c), however, results in a deviation from the Mignolet hysteresis. In the first half-cycle (point A to point B), the steady-state hysteresis path is followed as usual, but load reversal occurs well before reaching the initial loading curve. The ring-down curve also reverses early after the second half-cycle (point C), and it is more apparent that the regime of linear force versus displacement (the path with constant slope just before point C) is shortening. This constant slope regime ultimately disappears, and the shape of the hysteresis in the third full-cycle (E to F to E) is completely different from the Mignolet hysteresis. As a result, in the ring down case shown here the secant slope (effective stiffness) would be in error by  $-14.8\%$  and the enclosed area (energy dissipated per cycle) would be in error by  $90.3\%$  of the values calculated from Mignolet's equations.

## 4 CONCLUSION

The results of Section 3.2 reveal an important caveat regarding Mignolet's steady-state assumptions for the five-parameter Iwan-type model. By allowing the kinetic friction force to be less than the maximum static friction force, the five-parameter model exhibits a form of history-dependence in that the shape of the hysteresis at lower amplitudes is controlled by that of the highest-achieved amplitude. The ring-down cycles in a general five-parameter model hardly resemble those of the Mignolet hysteresis, so, therefore, Mignolet's expressions for steady-state stiffness and dissipation cannot be used to estimate the same properties in a ring-down response. This demonstrates that Mignolet's steady-state stiffness and dissipation equations implicitly assume that the steady state was reached via a monotonically-increasing displacement amplitude.

In the conference presentation, further case studies will be presented and elaborated. Furthermore, dynamic simulations on the transient (ring-down) response of four- and five-parameter Iwan models will be presented, showing that the response of a system with a five-parameter model can be exactly represented with a four-parameter model after the amplitude decreases below the hysteretic regime of constant slope.

## REFERENCES

- [1] W. D. Iwan. A distributed-element model for hysteresis and its steady-state dynamic response. *Journal of Applied Mechanics*, 33(4):893–900, 1966.
- [2] D. J. Segalman. A four-parameter Iwan model for lap-type joints. *Journal of Applied Mechanics*, 72(5):752–760, 2005.
- [3] Robert M. Lacayo and Matthew S. Allen. Updating structural models containing nonlinear Iwan joints using quasi-static modal analysis. *Mechanical Systems and Signal Processing*, 118:133–157, 2019.
- [4] Brandon J. Deaner, Matthew S. Allen, Michael J Starr, Daniel J Segalman, and Hartono Sumali. Application of viscous and iwan modal damping models to experimental measurements from bolted structures. *Journal of Vibration and Acoustics*, 137(2):021012, 2015.
- [5] Daniel R. Roettgen and Matthew S. Allen. Nonlinear characterization of a bolted, industrial structure using a modal framework. *Mechanical Systems and Signal Processing*, 84, Part B:152–170, 2017.
- [6] Robert M. Lacayo, Brandon J. Deaner, and Matthew S. Allen. A numerical study on the limitations of modal Iwan models for impulsive excitations. *Journal of Sound and Vibration*, 390:118–140, 2017.
- [7] Marc P. Mignolet, Pengchao Song, and X. Q. Wang. A stochastic Iwan-type model for joint behavior variability modeling. *Journal of Sound and Vibration*, 349:289–298, 2015.
- [8] Robert Lacayo, Luca Pesaresi, Johann Gross, Daniel Fochler, Jason Armand, Loic Salles, Christoph Schwingshackl, Matthew Allen, and Matthew Brake. Nonlinear modeling of structures with bolted joints: A comparison of two approaches based on a time-domain and frequency-domain solver. *Mechanical Systems and Signal Processing*, 114:413–438, 2019.